I S A V

Journal of Theoretical and Applied

Vibration and Acoustics

journal homepage: http://tava.isav.ir

Nondestructive thickness mapping of corroded plate structures using guided lamb wave propagation

Seyed Alireza Azimi, Ali Mardanshahi, Siavash Kazemirad*

School of Mechanical Engineering, Iran University of Science and Technology, Tehran, Iran

ARTICLE INFO

Article history:
Received 14 February 2021

Received in revised form
5 March 2021

Accepted 23 April 2021

Available online 29 April 2021

Keywords:
Ultrasound

NDE

Corrosion

Guided wave tomography

ABSTRACT

Nondestructive evaluation (NDE) of thickness loss in plate structures is an important monitoring task. A two-step NDE method for rapid and reliable corrosion mapping of plate structures using the Lamb wave propagation is proposed in this study. The analytical model for thickness mapping via the Lamb wave propagation was presented. One strip and one plate specimen with varying thickness profiles were fabricated from steel and then tested. The A_0 Lamb wave mode was propagated in the fabricated specimens with an excitation frequency of 60 kHz. The Lamb wave velocity and thus the Lamb wavenumber were first measured experimentally, which were used to estimate the thickness of the specimens for each measurement span from the numerical solution of the presented Lamb wave propagation model. The approximate mean thickness of the specimens within the corrosion zone was estimated in the first measurement step, while the mapping of the thickness profile of the corrosion zone was performed in the second measurement step. The mean thickness and the thickness profile of the corrosion zone estimated from the proposed method were found to be in good agreement with the actual mean thickness and thickness profile for both of the strip and plate specimens. Thus, it was concluded that the proposed Lamb wave propagation method can be utilized as a strong nondestructive evaluation tool for rapid thickness mapping of corroded plate structures.

1. Introduction

Metal plates are used in many engineering applications. The rapid and reliable inspection of the plate structures is thus an important monitoring task to ensure their integrity. Corrosion is the gradual decay of metal structures by chemical or electrochemical reactions with the environment [1]. The safety and performance of metal plates are highly impacted by corrosion. The accurate

* Corresponding author:
E-mail address: skazemirad@iust.ac.ir (S. kazemirad)

http://dx.doi.org/10.22064/tava.2022.540517.1194

nondestructive and in-situ assessment of the corrosion-induced thickness loss of metal plate structures in oil tanks and pressure vessels in petrochemical industries is for example highly demanded. The A-scan ultrasonic thickness measurements that are conventionally used in industrial applications need to be performed at every desired spot of the structure. Thus, this method does not offer the potential for rapid evaluation of corroded structures.

The high frequency and low attenuation nature of Lamb waves compared to the vibration-based inspection methods allows them to be used for in-situ and rapid evaluation of different types of structures. Nondestructive evaluation (NDE) and characterization of plate structures have extensively been performed in prior research works via the Lamb wave propagation [2-14]. For example, Yelve et al. in [14] proposed a Lamb wave propagation for the detection of delamination damage in composite specimens. Gao et al. in [6] developed a method using the propagation of A_0 Lamb wave mode to identify the size and location of delamination and disbonding damage in composite materials. Fathi et al. in [5] proposed a combined Lamb wave propagation and machine learning approach for the prediction of the mechanical properties of wood. Mardanshahi et al. in [9] developed a Lamb wave propagation method for the characterization of the viscoelastic properties of polymeric composites with the purpose of nondestructive identification of matrix cracking in them.

The thickness measurement and corrosion mapping of plate structures has been performed using the Lamb wave propagation in the literature [4, 15-21]. For instance, Jenot et al. in [18] used the group velocity of the S_0 Lamb wave mode for the assessment of thickness loss in plate structures. Only a specific corrosion area and constant thickness loss at each corrosion step were considered in their study and no corroded specimens with varying thickness profiles were investigated. Michaels and Michaels in [19] assessed the detection of corrosion in aluminum plates and the identification of the size of the defects using the Lamb wave propagation. Bingham et al. in [15] inspected the corrosion-thinning in aircraft stringers using the Lamb wave propagation. They observed that the A_0 Lamb wave mode is more sensitive to the corroded surface than the S_0 Lamb wave mode. Howard and Cegla in [16, 17] examined the detection of pipe wall thinning using the A_0 and S_0 Lamb wave modes and estimated the defects' location and size. In none of the above-mentioned studies, the thickness mapping (tomography) of the corroded area was performed. Rao et al. in [21] proposed a Lamb wave tomography method for corrosion mapping of plate structures. An array consisting of a huge number (60) of piezoelectric stack transducers was used for the corrosion detection and thickness mapping of the corroded zone. As seen in the above-mentioned review of prior research works, the accurate and rapid in-situ assessment of the thickness map of corroded metal plates has remained challenging.

The aim of this study was to develop a two-step nondestructive evaluation method for reliable and rapid thickness mapping of corroded plate structures based on the guided Lamb wave propagation method. The analytical model of the Lamb wave propagation tomography was presented. One strip and one plate specimen with varying thickness profiles were fabricated from steel and tested. In the first measurement step, the corrosion zone and the approximate mean thickness of the specimens within this zone were estimated. In the second step, the thickness mapping of the corrosion zone was performed and its thickness profile was obtained. This two-step evaluation method allows the rapid assessment of the uncorroded area and the accurate thickness mapping of the corroded area. The thickness profiles of the specimens estimated via the proposed method were compared with the actual thickness profiles for the verification purpose.

2. Methods

2.1. Fabrication of the specimens

One strip and one plate specimen were fabricated from the ST37 carbon steel for the Lamb wave propagation tomography experiments in this study. The dimensions of the strip specimen were initially 300×30×3 mm. A circular curve thickness profile was made in the middle of the strip specimen using a computer numerical control (CNC) milling machine. The thickness of the strip specimen was 1 mm at its center. The strip specimen's thickness gradually increased and became 3 mm at a distance of 50 mm from its center, as shown in Figure 1. The plate specimen was used to evaluate the performance of the proposed tomography and thickness mapping method using the lamb wave propagation on plate structures. The dimensions of the plate specimen were initially 300×30×30 mm. A convex thickness profile with a diameter of 150 mm and a minimum thickness of 1 mm at the center of the profile was made in the middle of the plate structure using a CNC milling machine as shown in Figure 2. The thickness profiles made in the strip and plate specimens using the CNC milling machine were designed in CAD software, thus the actual thickness of each spot of the specimens was known. To assess the accuracy of the milling process, the thickness of several spots of the specimens was measured using a caliper, which confirmed the accuracy of the process.

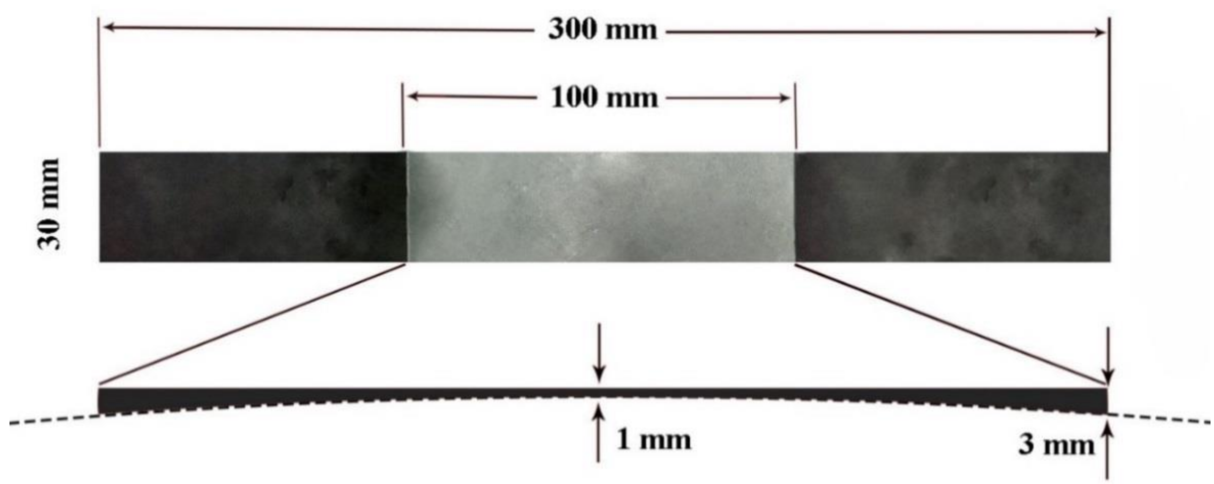

Fig 1. The geometry of the fabricated strip specimen.

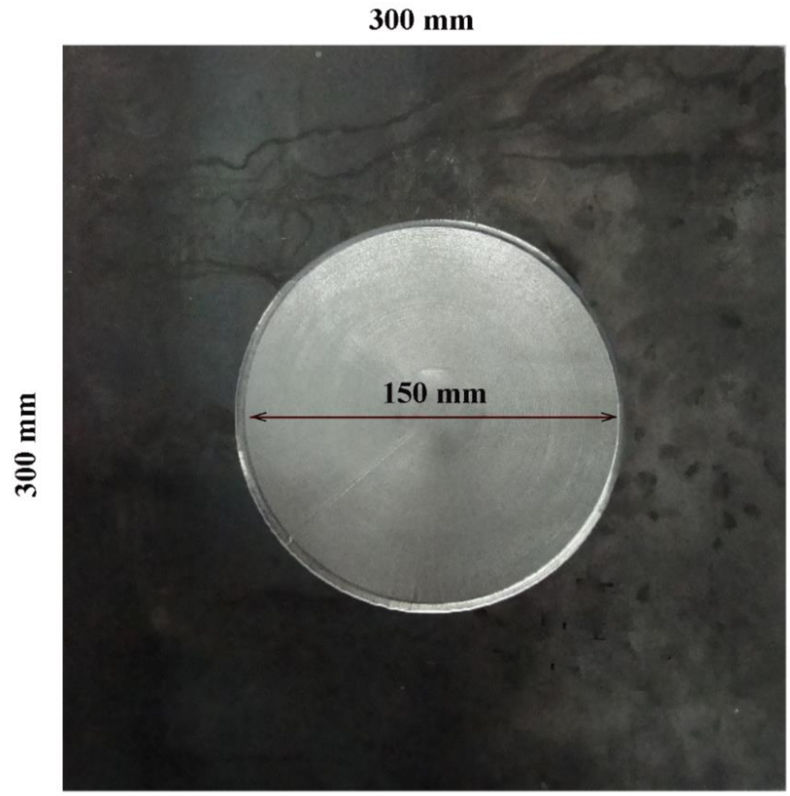

Fig 2. The fabricated plate specimen and the convex thickness profile made in it.

2.2. Lamb wave propagation in elastic plates

The Lamb waves are generated by the interaction of the longitudinal and shear waves in plate-like structures. The steel strip and plate specimens fabricated and tested in this study were assumed to be macroscopically homogeneous and elastic. Therefore, the Navier equation for homogeneous elastic materials governs the wave propagation in the specimens. The decomposition of the Navier equation and application of proper boundary conditions lead to the governing relation for the antisymmetric Lamb wave mode as [22]:

$$\frac{\tanh(\eta h)}{\tanh(\beta h)} = \frac{4k_L^2\eta\beta}{(2k_L^2 - k_s^2)^2} \tag{1}$$

where h is half of the specimen's thickness and k_L, k_s, and k_c are the Lamb, shear, and longitudinal wavenumbers, respectively. Furthermore, η and β are obtained via:

$$\eta^2 = k_L^2 - k_c^2 \tag{2}$$

$$\beta^2 = k_L^2 - k_s^2 \tag{3}$$

The mechanical properties of the specimens and thus the shear and longitudinal wavenumbers were known in this study. The A_0 Lamb wave mode was propagated in the fabricated strip and plate specimens. In this case, the Lamb wave velocity and consequently the Lamb wavenumber (k_L) was first obtained experimentally, using which the thickness of the specimens was estimated for each measurement span by solving Eq. (4) numerically.

2.3. Lamb wave propagation experiments

The Lamb wave propagation experiments were carried out on the strip and plate specimens. The experimental setup used for this purpose consisted of a wave function generator (Owon AG1022F), a digital oscilloscope (Owon TDS7104), a computer, a 60 kHz ultrasonic actuator with a diameter of 30 mm, and two high sensitivity ultrasonic sensors with a diameter of 50 mm and a center frequency of 206 kHz that were shown to work properly at the frequency range from 40 kHz to 500 kHz.

The dispersion curves corresponding to the A_0 and S_0 Lamb wave modes for the ST37 carbon steel specimens are shown in Figure 3. These curves were estimated and plotted via the GUIGUW_V2.2 software. As it is seen in this figure, the slope of the dispersion curve for the A_0 Lamb wave mode was higher than that for the S_0 Lamb wave mode in the frequency×thickness range of up to 1500 kHz.mm. Therefore, the A_0 Lamb wave mode was selected for the thickness measurement of the strip and plate specimens in this study, as a higher slope in the dispersion curve yields a higher sensitivity of the measurements to the thickness variations. Furthermore, the slope of the dispersion curve for the A_0 Lamb wave mode was higher at low frequency×thickness, for instance lower than 200 kHz.mm. Therefore, the excitation frequency was set to 60 kHz in this study, so that the maximum frequency×thickness was 180 kHz.mm at the thickness of 3 mm and smaller than 180 kHz.mm in the corrosion zone.

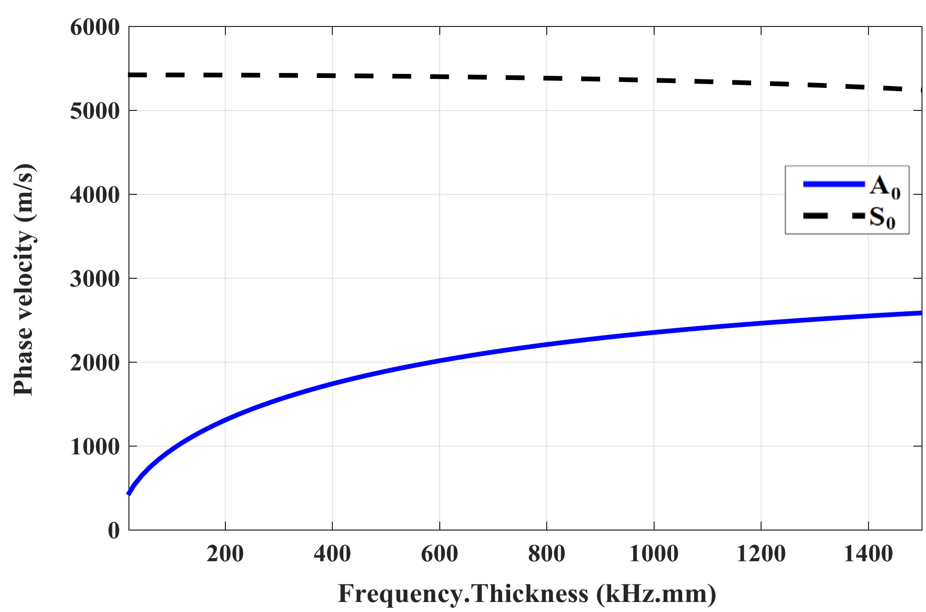

Fig 3. The dispersion curves corresponding to the A_0 and S_0 Lamb wave modes for the ST37 carbon steel specimens plotted via the GUIGUW software.

The A_0 Lamb wave mode with a sinusoidal waveform and a frequency of 60 kHz was generated in the strip and plate specimens using the ultrasonic actuator that was connected to the function generator. In order to assure the rapid assessment of the uncorroded area and accurate thickness mapping of the corroded area, a two-step NDE process was proposed. Therefore, the Lamb wave propagation measurements were performed in two steps for both of the strip and plate specimens. In each measurement step explained in the following, the Lamb wave signals were acquired through the two high sensitivity sensors and the Lamb wave velocity (c_L) was estimated for different specific locations (spans between the two sensors) on the specimens through the phase difference of the Lamb wave signals acquired using the two sensors.

In the first measurement step for the strip specimen, the Lamb wave signals were acquired using the two sensors connected to the digital oscilloscope, which were placed on the specimen with a center to center distance of 120 mm. The two ultrasonic sensors were placed at the two sides of the circular curve thickness profile made in the middle of the strip specimen. The phase velocity for the span between the two ultrasonic sensors was estimated through the measurement of the phase difference of the signals received by the two sensors. Consequently, the approximate mean thickness of the specimen for the span between the two sensors was estimated using the measured phase velocity. The purpose of performing the first measurement step in the proposed two-step NDE method was to rapidly identify the corrosion zone, where the overall (mean) thickness is smaller than that for the uncorroded area. In the second step, the two sensors with a fixed center to center distance of 55 mm were moved on the specimen along the wave propagation direction. The thickness mapping of the corrosion zone was performed in this step and its thickness profile was obtained. Figure 4 shows the setup used for the Lamb wave propagation experiments on the strip specimen.

In the first measurement step for the plate specimen, the ultrasonic actuator was placed near one corner of the specimen and the two ultrasonic sensors were placed on the two sides of the convex thickness profile in radial directions along the wave propagation path with a center to center distance of 190 mm. The mean thickness of the plate specimen within the corrosion zone was estimated on each of these radial paths.

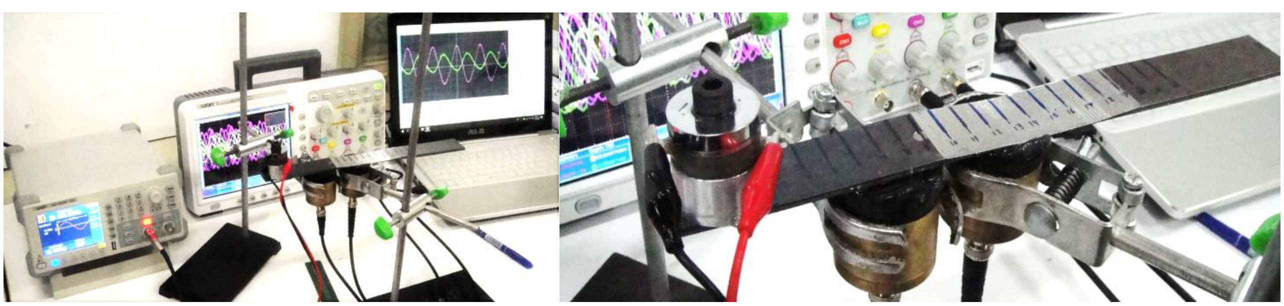

(a) (b)

Fig 4. (a) The setup used for the Lamb wave propagation experiments on the strip specimen, and (b) the configuration of the actuator and sensors.

(a)

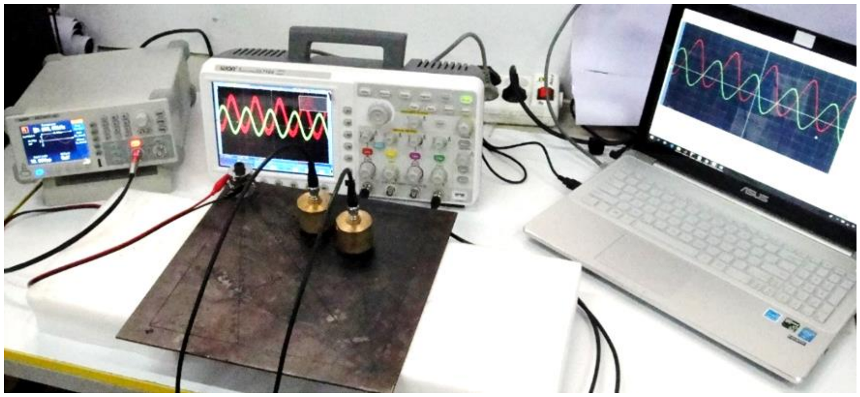

(b)

(c)

Fig 5. (a) The setup used for the Lamb wave propagation experiments on the plate specimen, and the configuration of the actuator and sensors for the measurements on (b) the radial directions and (c) the vertical directions

The second measurement step for the plate specimen was performed in two different manners. First, the ultrasonic actuator was placed near one corner of the specimen and the two sensors with a fixed center to center distance of 55 mm were moved on the plate specimen along the wave propagation direction in the radial directions with respect to the actuator. Second, the ultrasonic actuator was placed near the two edges of the specimen and the two sensors with a fixed center to center distance of 55 mm were moved along the wave propagation path and acquired the Lamb wave signals in the vertical directions perpendicular to two adjacent edges of the plate specimen. Figure 5 shows the setup used for the Lamb wave propagation experiments on the strip specimen.

It is worth mentioning that the sampling rate of the oscilloscope was set to 10 MSamples/s for all Lamb wave propagation measurements. To ensure the proper coupling between the two sensors and the strip and plate specimens, an ultrasonic gel was applied on the surface of the specimens. As mentioned before, the Lamb wave velocity (c_L) for each measurement on the strip and plate specimens was obtained via the phase difference of the Lamb wave signals at different locations along the propagation directions. The Lamb wavenumber (k_L) was then calculated using the obtained Lamb wave velocity for each measurement. The thickness of the specimens was eventually estimated for each measurement step and span through the numerical solution of the analytical model given in the previous subsection.

3. Results and discussion

Typical wave signals acquired from the plate specimen at different distances between the actuator and sensors are shown in Figure 6. It was observed that strong and relatively noise-free signals were acquired using the high-sensitivity sensors used in this study. As seen in Figure 6, the wave amplitude decreased with the propagation distance.

Table 1 presents the phase velocity and wavelength of A_0 Lamb wave mode, the actual mean thickness of the corrosion zone, and the estimated approximate mean thickness obtained from the first measurement step for the strip specimen, in which the two ultrasonic sensors were placed at the two sides of the circular curve thickness profile made in the middle of the strip specimen. As seen in Table 1, the mean thickness of the corrosion zone estimated from the Lamb wave propagation measurement was in good agreement with the actual mean thickness of the corrosion zone with a difference of 8.6%. It proves the ability of the Lamb wave propagation measurements proposed in this study for rapid assessment of metal structures to identify the corrosion zone and estimate the approximate thickness loss. The minor difference between the actual and experimentally obtained mean thickness may be due to the Lamb wave propagation measurement and post-processing procedure. Moreover, the wavelength of the Lamb wave propagated in the specimen was 15.9 mm, which was perhaps not small enough to detect sudden thickness variations in the specimen. Smaller wavelengths can be achieved at higher excitation frequencies. However, the slope of the dispersion curve for the A_0 Lamb wave mode decreases at higher frequencies. Therefore, the selected excitation frequency for the measurements performed in this study seems to be reasonable.

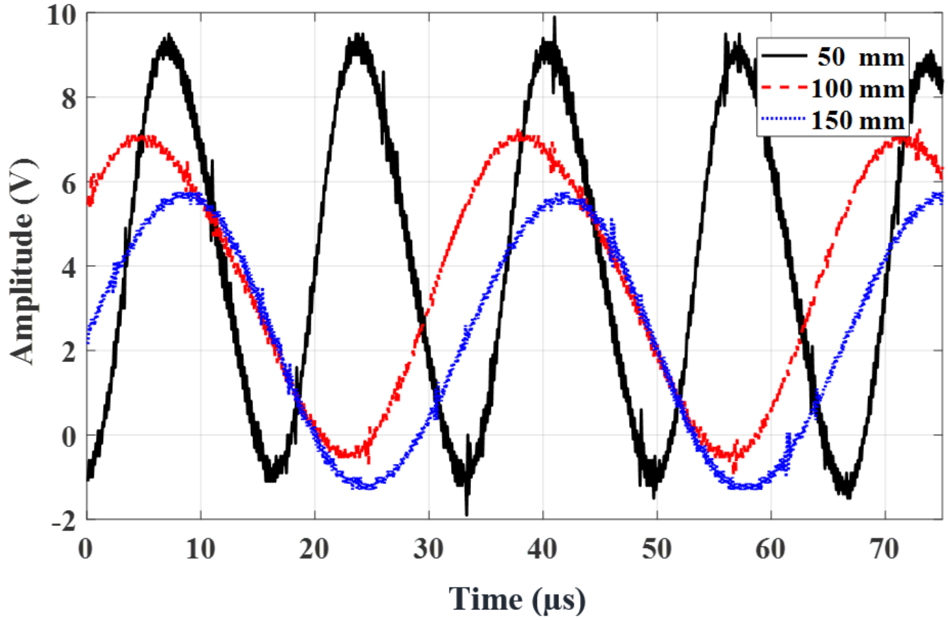

Fig 6. Typical wave signals acquired from the plate specimen at different distances between the actuator and sensors.

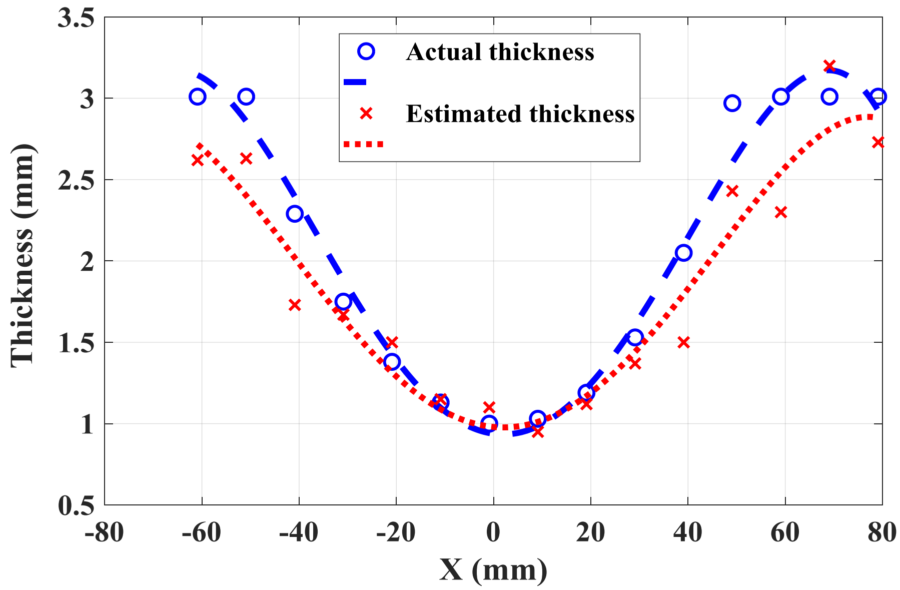

Fig 7. The actual thickness profile of the circular curve made in the middle of the strip specimen and the one that was estimated from the second step of the Lamb wave propagation measurements.

Table 1. The phase velocity and wavelength of A_0 Lamb wave mode, the actual mean thickness of the corrosion zone, and the estimated approximate mean thickness were obtained from the first measurement step for the strip specimen.

Phase velocity (m/s)	Wavelength (mm)	Estimated thickness (mm)	Actual thickness (mm)	Error (%)
958	15.9	1.70	1.86	8.6

The actual thickness profile of the circular curve made in the middle of the strip specimen and that estimated from the second step of the Lamb wave propagation measurements are illustrated in Figure 7. It is seen that the thickness mapping of the corrosion zone was carried out via the proposed Lamb wave propagation method with an acceptable accuracy, where the average difference between the actual thicknesses and the experimentally estimated thicknesses within the corrosion zone was about 11%. It reveals that the Lamb wave propagation method may be capable of accurate thickness mapping of corroded structures. The minimum discrepancy between the actual and estimated thickness was about 1% which occurred in the middle of the corrosion zone (minimum thickness), while the maximum discrepancy was about 23% and belonged to the two sides of the circular curve corrosion profile. The diameter of the high-sensitivity ultrasonic sensors used in this study was near 50 mm. Therefore, the minimum center to center distance between the sensors could be set to about 55 mm. Consequently, when the two sensors with a fixed center to center distance of 55 mm were moved on the strip specimen along the wave propagation direction, only the mean thickness within each span of 55 mm length was obtained. Thus, the sudden thickness change in the two sides of the corrosion zone was not detected accurately. The use of high-sensitivity ultrasonic sensors with smaller diameters may help to overcome this limitation.

The results of the first measurement step for the plate specimen, in which the actuator was placed near one corner of the specimen and the two sensors were placed on the two sides of the convex thickness profile in radial directions along the wave propagation path, showed that the mean thickness of the corrosion zone estimated form the Lamb wave propagation measurements was in good agreement with the actual mean thickness with a difference of 6.3%. Similar to the case of the strip specimen, the Lamb wave propagation method was shown to be capable of rapid evaluation of plate metal structures to identify the corrosion zone and estimate the approximate thickness loss was proven. A surface shell was fitted to the actual thickness of the convex corrosion profile in the plate specimen, which is shown in Figure 8 (a). The estimated thicknesses of different points of the convex corrosion profile of the plate specimen acquired by the second step of the Lamb wave propagation measurements on the radial paths and the surface shell fitted to them are also shown in Figure 8 (b). As shown in this figure, the convex thickness profile of the corrosion zone was properly detected by the second step of the Lamb wave propagation measurements. The average difference between the actual thicknesses and the experimentally estimated thicknesses within the corrosion zone from the radial Lamb wave propagation measurements was 5.8%. Similar observations were made for the second step of the Lamb wave propagation measurements on the vertical paths to estimate the thickness of different points of the convex corrosion profile (not shown here), in which the average difference between the actual thicknesses and the experimentally estimated thicknesses was 2.5%. The difference between the actual and experimentally estimated thicknesses of the corrosion zone for the plate specimen obtained from both the radial and vertical direction measurements was interestingly smaller than that for the strip specimen (11%). It may be due to the smaller wave reflections from the plate specimen boundaries compared to that for the strip specimen. It led to a higher signal-to-noise ratio for the signals obtained from the plate specimen, and thus a better estimation of the Lamb wave phase velocity and the specimen's thickness.

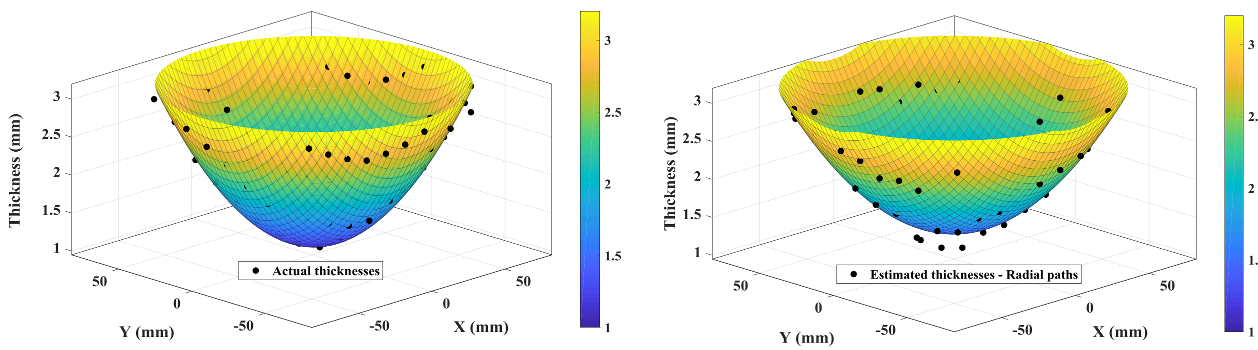

(a) **(b)**

Fig 8. (a) The surface shell fitted to the actual thickness of the convex corrosion profile in the plate specimen, and (b) the experimentally estimated thicknesses of the convex corrosion profile in the plate specimen and the surface shell fitted to them.

To better illustrate and compare the actual and experimentally estimated thickness profiles of the convex corrosion zone in the plate specimen, a cross-section of the thickness profile in the Y-Z plane (X=0) is depicted in Figure 9. It is seen that the minimum difference between the actual and estimated thicknesses was less than 1% for both the radial and vertical path measurements, which occurred in the middle of the corrosion zone (minimum thickness). The maximum difference between the actual and estimated thicknesses was about 6% and 20% for the vertical and radial paths, respectively, and obtained at the two sides of the cross-section of the corrosion profile. Similar to the case of the strip specimen, the sudden thickness change in the two sides of the corrosion zone in the plate specimen was not detected accurately. It was also observed that the Lamb wave propagation measurements on the vertical paths yielded a smaller error in the estimation of the thickness of the convex corrosion profile. One reason for this observation may be the fact that the measurement locations were evenly distributed on the surface of the plate specimen in the case of the vertical path measurements, while in the case of the radial path measurements there were a higher number of the measurement locations close to the actuator and a smaller number of the measurement locations far from the actuator. However, the application of the Lamb wave measurements on the radial paths for the thickness mapping of corroded plates is superior to that on the vertical paths with respect to the measurement time and complexity, as there is no need to change the location of the ultrasonic actuator on the specimen surface in the case of the radial path measurements.

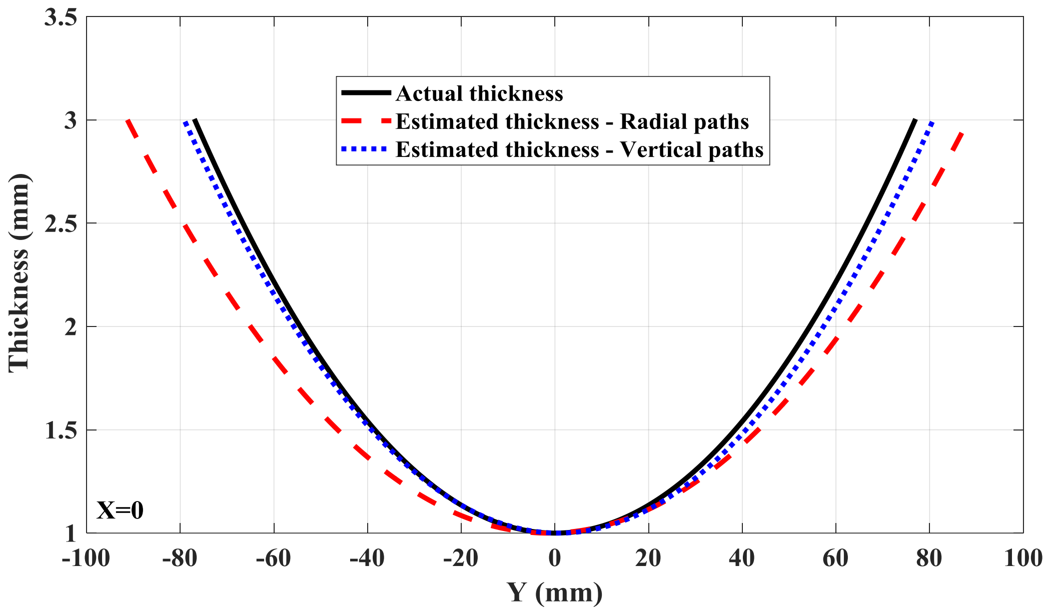

Fig 9. A cross-section of the actual thickness profile in the Y-Z plane (X=0) in the middle of the plate specimen and the one that was estimated from the second step of the Lamb wave measurements on the radial and vertical paths.

This study had limitations. For example, Eq. (4) is the governing relation for the propagation of the antisymmetric Lamb wave mode in plate structures with a uniform thickness of $2h$. Therefore, the approximate mean (overall) thickness of the corrosion zone and the approximate thickness profile (thickness at different specific spots) of the circular curve and convex made in the strip and plate specimens were estimated from the first and second measurements steps, respectively. In the second measurement step, for instance, it was assumed that the thickness was constant over the spans of 55 mm long between the two sensors, which indeed induced some error in the obtained results. However, the reported difference between the estimated and actual mean thickness and thickness profile of the strip and plate specimens proved the validity of the assumption made and the accuracy of the results obtained in this study.

4. Conclusion

A two-step nondestructive evaluation method was proposed in this study using the Lamb wave propagation for reliable and rapid corrosion mapping in plate structures. The analytical model was presented for thickness mapping via the Lamb wave propagation. One strip and one plate specimen with varying thickness profiles were made of steel. The A_0 Lamb wave mode with a frequency of 60 kHz was propagated in the fabricated specimens. The excited Lamb wave mode and frequency were selected in a way to assure a relatively high slope in the dispersion curve, which offered a high sensitivity of the measurements to the variations in the specimens' thickness. The mean thickness and thickness profile of the corrosion zone estimated from the Lamb wave propagation measurements were found to be in good agreement with the actual mean thickness and thickness profile for both the strip and plate specimens. It was observed that the sudden thickness change in the two sides of the corrosion zone was not detected accurately for the strip and plate specimens. Moreover, the Lamb wave propagation measurements on the vertical paths yielded a lower error in the thickness mapping of the corrosion zone in the plate specimen. However, the thickness mapping of corroded plate structures on the radial paths may be faster and easier to perform. In conclusion, the developed two-step Lamb wave propagation method was shown to be capable of rapid nondestructive assessment of plate structures to identify the corrosion zone and estimate their thickness loss.

References

[1] Z. Ahmad, Principles of corrosion engineering and corrosion control, Elsevier, 2006.

[2] D. Barazanchy, V. Giurgiutiu, A unified formulation for predictive modeling of guided-ultrasonic wave dispersion curves in metallic and composite materials, Journal of Intelligent Material Systems and Structures, 28 (2017) 1272-1286.

[3] H. Cho, M. Hasanian, S. Shan, C.J. Lissenden, Nonlinear guided wave technique for localized damage detection in plates with surface-bonded sensors to receive Lamb waves generated by shear-horizontal wave mixing, NDT & E International, 102 (2019) 35-46.

[4] A. Ebrahiminejad, A. Mardanshahi, S. Kazemirad, Nondestructive evaluation of coated structures using Lamb wave propagation, Applied Acoustics, 185 (2022) 108378.

[5] H. Fathi, V. Nasir, S. Kazemirad, Prediction of the mechanical properties of wood using guided wave propagation and machine learning, Construction and Building Materials, 262 (2020) 120848.

[6] F. Gao, L. Zeng, J. Lin, Y. Shao, Damage assessment in composite laminates via broadband Lamb wave, Ultrasonics, 86 (2018) 49-58.

[7] W. Li, Y. Cho, J.D. Achenbach, Detection of thermal fatigue in composites by second harmonic Lamb waves, Smart Materials and Structures, 21 (2012) 085019.

[8] A. Mardanshahi, V. Nasir, S. Kazemirad, M. Shokrieh, Detection and classification of matrix cracking in laminated composites using guided wave propagation and artificial neural networks, Composite Structures, 246 (2020) 112403.

[9] A. Mardanshahi, M. Shokrieh, S. Kazemirad, Identification of matrix cracking in cross-ply laminated composites using Lamb wave propagation, Composite Structures, 235 (2020) 111790.

[10] A. Mardanshahi, M. Shokrieh, S. Kazemirad, Simulated Lamb wave propagation method for nondestructive monitoring of matrix cracking in laminated composites, Structural Health Monitoring, (2021) 14759217211008620.

[11] F. Masurkar, P. Tse, N.P. Yelve, Evaluation of inherent and dislocation induced material nonlinearity in metallic plates using Lamb waves, Applied Acoustics, 136 (2018) 76-85.

[12] H. Ramezani, S. Kazemirad, M. Shokrieh, A. Mardanshahi, Effects of adding carbon nanofibers on the reduction of matrix cracking in laminated composites: Experimental and analytical approaches, Polymer Testing, 94 (2021) 106988.

[13] E. Rosenkrantz, A. Bottero, D. Komatitsch, V. Monteiller, A flexible numerical approach for non-destructive ultrasonic testing based on a time-domain spectral-element method: Ultrasonic modeling of Lamb waves in immersed defective structures and of bulk waves in damaged anisotropic materials, NDT & E International, 101 (2019) 72-86.

[14] N.P. Yelve, M. Mitra, P. Mujumdar, Detection of delamination in composite laminates using Lamb wave based nonlinear method, Composite Structures, 159 (2017) 257-266.

[15] J. Bingham, M. Hinders, Lamb wave characterization of corrosion-thinning in aircraft stringers: Experiment and three-dimensional simulation, The Journal of the Acoustical Society of America, 126 (2009) 103-113.

[16] R. Howard, F. Cegla, Detectability of corrosion damage with circumferential guided waves in reflection and transmission, NDT & E International, 91 (2017) 108-119.

[17] R. Howard, F. Cegla, On the probability of detecting wall thinning defects with dispersive circumferential guided waves, NDT & E International, 86 (2017) 73-82.
[18] F. Jenot, M. Ouaftouh, M. Duquennoy, M. Ourak, Corrosion thickness gauging in plates using Lamb wave group velocity measurements, Measurement Science and Technology, 12 (2001) 1287.
[19] T.E. Michaels, J.E. Michaels, Monitoring and characterizing corrosion in aluminum using Lamb waves and attached sensors, in: Health monitoring of structural and biological systems 2007, SPIE, 2007, pp. 487-497.
[20] E. Moreno, P. Acevedo, Thickness measurement in composite materials using Lamb waves, Ultrasonics, 35 (1998) 581-586.
[21] J. Rao, M. Ratassepp, D. Lisevych, M. Hamzah Caffoor, Z. Fan, On-line corrosion monitoring of plate structures based on guided wave tomography using piezoelectric sensors, Sensors, 17 (2017) 2882.
[22] T. Kundu, Ultrasonic nondestructive evaluation: engineering and biological material characterization, CRC press, 2003.